Journal of Experimental Botany, Vol. 64, No. 8, pp. 2359–2372, 2013
doi:10.1093/jxb/ert093
This paper is available online free of all access charges (see http://jxb.oxfordjournals.org/open_access.html for further details)

Journal of Experimental Botany
www.jxb.oxfordjournals.org

RESEARCH PAPER

Zm908p11, encoded by a short open reading frame (sORF) gene, functions in pollen tube growth as a profilin ligand in maize

Xue Dong, Dongxue Wang*, Peng Liu†, Chengxia Li‡, Qian Zhao, Dengyun Zhu and Jingjuan Yu§

State Key Laboratory for Agrobiotechnology, College of Biological Sciences, China Agricultural University, Beijing 100193, China
* Present address: Department of Biology, Emory University, Atlanta, GA 30322, USA.
† Present address: Laboratory of Plant Molecular Biology, Rockefeller University, NY 10065, USA.
‡ Present address: Department of Plant Sciences, University of California, Davis, CA 95616, USA.

§ To whom correspondence should be addressed. E-mail: yujj@cau.edu.cn

Received 19 November 2012; Revised 24 February 2013; Accepted 5 March 2013

Abstract

Double fertilization of flowering plants depends on the targeted transportation of sperm to the embryo sac by the pollen tube. Currently, little is known about the underlying molecular mechanisms that regulate pollen germination and pollen tube growth in maize (*Zea mays*). Here, a maize pollen-predominant gene *Zm908*, with several putative short open reading frames (sORFs), was isolated and characterized. The longest ORF of *Zm908* encodes a small protein of 97 amino acids. This was designated as Zm908p11 and is distributed throughout the maize pollen tube. Western blot detected the small peptide in mature pollen. Quantitative reverse transcription–PCR and northern blot analysis revealed that *Zm908p11* was expressed predominantly in mature pollen grains. Ectopic overexpression of full-length *Zm908* and *Zm908p11* in tobacco resulted in defective pollen, while transgenic tobacco plants with a site-specific mutation or a frameshift mutation of *Zm908p11* showed normal pollen development. Overexpression of *Zm908p11* in maize decreased pollen germination efficiency. Maize pollen cDNA library screening and protein–protein interaction assays demonstrated that Zm908p11 interacts with maize profilin 1 (ZmPRO1). A microarray analysis identified 273 up-regulated and 203 down-regulated genes in the overexpressing transgenic *Zm908p11* pollen. Taken together, these results indicate that *Zm908* functions as Zm908p11, and binds to profilins as a novel ligand, with a required role during pollen tube growth in maize. Accordingly, a model is proposed for the role of Zm908p11 during pollen tube growth in maize.

Key words: pollen tube, pollen-predominant, profilin, short open reading frame, *Zea mays*, *Zm908p11*.

Introduction

In flowering plants, male gametophyte (pollen) development is a complicated biological process. It takes place in the anther locules and comprises two essential phases: microsporogenesis and microgametogenesis (Borg *et al.*, 2009). The mature pollen grain of maize (*Zea mays*) consists of three cells: two small sperm cells and a larger vegetative cell. After the pollen grain arrives at the compatible stigmatic hairs of maize silk, it hydrates. The pollen tube then starts to elongate in the style, which connects the stigma to the embryo sac. Ultimately, the sperm cells are delivered into the embryo sac of an ovule to achieve double fertilization. One sperm cell fuses with the egg cell, giving rise to the zygote, while the other one fuses with the central cell and develops into the primary endosperm (Mascarenhas, 1990; Taylor and Hepler, 1997).

Processes that control pollen germination and tube growth involve multiple signal transduction molecules, including Ca^{2+} (Holdaway-Clarke and Hepler, 2003), calmodulin (CaM; Moutinho *et al.*, 1998), phosphoinositides (Moutinho *et al.*, 2001), and GTPase (Cheung *et al.*, 2002). These modulate vesicle targeting and the physical state of the actin cytoskeleton required for tube elongation (Miller *et al.*, 1996). The actin cytoskeleton is a highly organized dynamic structure that plays prominent roles in pollen germination and tube growth. Specific roles include organelle positioning (Kadota *et al.*, 2009), cytoplasmic streaming (Cárdenas *et al.*, 2005), vesicle trafficking (Kim *et al.*, 2005), and polar growth (Vidali *et al.*, 2001). Various actin-binding proteins (ABPs) are involved in the regulation of actin dynamics, and these have the ability to bind to actin monomer and/or actin filaments (Higaki *et al.*, 2007). ABPs regulate actin dynamics by maintaining the steady-state equilibrium between actin monomers and actin filaments (Staiger *et al.*, 2010). In flowering plants, a subset of ABPs has been characterized from pollen (Lopez *et al.*, 1996; Staiger *et al.*, 1997), and includes actin-depolymerizing factors (ADFs) and profilins; these have similar or opposite effects on actin dynamics. ADFs bind to actin monomers and filaments, and preferentially depolymerize actin filaments by a complex mechanism. Increased levels of ADF in pollen tubes inhibit pollen tube growth and disrupt the actin cytoskeleton (Chen *et al.*, 2002). Profilins are actin monomer-binding proteins that are able to regulate actin nucleation, causing either actin polymerization or depolymerization (Perelroizen *et al.*, 1996; Kang *et al.*, 1999). Profilins, whose activity is dependent on the Ca^{2+} concentration, are distributed throughout the pollen tube (Kovar *et al.*, 2000). Five profilins have been identified in the maize PRO family (ZmPRO1–ZmPRO5). Of these, the *ZmPRO1, 2,* and *3* genes are highly expressed in pollen (Staiger *et al.*, 1993; Gibbon *et al.*, 1998; Kovar *et al.*, 2000). Additionally, profilin can bind to polyphosphoinositides, poly-L-proline (PLP), proline-rich proteins, and several multiprotein complexes to regulate actin nucleation (Fedorov *et al.*, 1994; Reinhard *et al.*, 1995; Mahoney *et al.*, 1999). Formins are a class of profilin-interactng proteins, which are a primary actin filament nucleation factors, and comprise two formin-homology domains, FH1 and FH2. The FH1 domain contains a proline-rich stretch which interacts with profilin and profilin–actin (Kovar *et al.*, 2006). The FH2 domain is necessary for actin filament nucleation (Zigmond, 2004).

In recent years, it has been reported that a novel class of small peptide genes are involved in plant morphogenesis processes, including organ growth and development. They contain one or more short open reading frames (sORFs) of <100 amino acid residues that are able to translate small peptides (Kastenmayer *et al.*, 2006). An increasing number of sORFs have been demonstrated to function as significant regulators in the control of cell proliferation, cell differentiation, and signal transduction in plants. For example, in the *Arabidopsis* mutant, *inflorescence deficient in abscission* (*ida*), the floral organs delay abscission after the shedding of mature seeds. This is because IDA is a ligand for the leucine-rich repeat receptor kinase HAESA, which influences floral organ abscission. *IDA* encodes a 77 amino acid protein with an N-terminal hydrophobic region, and is localized to the plasma membrane (Butenko *et al.*, 2003). In *Arabidopsis*, *CLAVATA3* (*CLV3*) encodes a 96 amino acid peptide with an 18 amino acid secretory signal peptide at the N-terminus. It has been reported that the *clv3* floral meristem is larger than that of the wild type, and forms a large mass of additional carpels, thus confirming that *CLV3* is a specific regulator in the coordination of cell differentiation and proliferation at the floral meristem throughout flower development (Clark *et al.*, 1995; Fletcher *et al.*, 1999). In addition to these, phytosulphokine-α (PSK-α) is a class of sulphated peptides. Its precursor peptide contains 80 amino acid residues and has a hydrophobic region at its N-terminus (Yang *et al.*, 1999). In pollen, PSK-α regulates cell surface receptors of pollen grains to influence density-dependent pollen germination and tube growth (Chen *et al.*, 2000).

By differential screening of the maize mature pollen cDNA library, two pollen-predominant genes with putative sORFs in maize were obtained, namely *Zm401* (AY911609) (Li *et al.*, 2001; Dai *et al.*, 2004) and *Zm908*. Alhough full-length *Zm401* is 1149 bp, the longest ORF is only 270 bp, and encodes the 89 amino acid peptide (~10 kDa) Zm401p10. *Zm401* plays a crucial role in the formation of Zm401p10 (Wang *et al.*, 2009). *In situ* hybridization demonstrated that *Zm401* is expressed specifically in tapetal cells and microspores (Ma *et al.*, 2008). Overexpression of *Zm401p10* causes retardation of tapetum degeneration and reduction of pollen viability (Wang *et al.*, 2009).

Here, another gene, *Zm908*, is studied. Functional analyses demonstrated that *Zm908* encodes a small functional peptide, Zm908p11 (with an estimated mol. wt of ~11 kDa). This peptide is localized throughout the pollen tube. Maize with overexpressed *Zm908p11* exhibited reduced pollen germination efficiency. This suggests that Zm908p11 functions in maize pollen germination. Protein–protein interaction assays revealed that Zm908p11 interacts with ZmPRO1. Moreover, transcript profiling data showed that overexpression of *Zm908p11* affects the expression of many genes involved in pollen tube growth. A possible mechanism for the involvement of *Zm908p11* in maize pollen germination and tube growth is discussed.

Materials and methods

Plant materials and growth conditions

Tobacco (*Nicotiana tabacum* cv Samsun NN and *Nicotiana benthamiana*) seeds were surface sterilized, and then sown on Murashige and Skoog (MS) solid medium (Murashige and Skoog, 1962) containing 3% sucrose and 0.8% agar. The plates were incubated at 28 °C under a 16 h light/8 h dark photoperiod for seed germination. The seedlings were then transferred to a bottle with the same medium and cultured under the same conditions as those for seed germination.

Maize inbred lines Z31 and Q31 were grown in a test field at China Agricultural University (Beijing). Immature embryos (~10 d after pollination) of the hybrid (Z31×Q31) were dissected and cultured on N6 solid medium containing 2% sucrose and 2.0 mg l^{-1} 2,4-D (pH 5.8) (Chu *et al.*, 1975) for callus induction in darkness at 28 °C, and subcultured every 14 d until transformation.

Constructs for tobacco transformation

Details of the construction are given in the Supplementary Materials and methods available at *JXB* online.

35S-Zm908s and 35S-Zm908a

The sense and antisense strands of the full-length *Zm908* were inserted into pBI121 between the *Cauliflower mosaic virus* (*CaMV*) *35S* promoter and the *Nos* terminator to generate *35S-Zm908s* (Supplementary Fig. S1A at *JXB* online) and *35S-Zm908a* (Supplementary Fig. S1B).

35S-Zm908p11, 35S-Zm908p11ss, and 35S-Zm908p11fs

The longest ORF, *Zm908p11* (+697 to +990), a site-specific mutation (the ATG start codon was replaced by AAG), and a frameshift mutation (the ATG start codon was replaced by ATGA) of *Zm908p11* were inserted into pBI121 between the *CaMV35S* promoter and the *Nos* terminator to generate *35S-Zm908p11s* (Supplementary Fig. S1C at *JXB* online), *35S-Zm908p11ss* (Supplementary Fig. S1D), and *35S-Zm908p11fs* (Supplementary Fig. S1E).

Lat52-Zm908s and Lat52-Zm908p11

The *CaMV35S* promoters in *35S-Zm908s* and *35S-Zm908p11* were replaced by the *Lat52* promoter to produce *Lat52-Zm908s* (Supplementary Fig. S1F at *JXB* online) and *Lat52-Zm908p11* (Supplementary Fig. S1G).

Constructs for maize transformation

Zm908p11 controlled by a 282 bp promoter fragment of *Zm908* (*Zm908p*) and the *Nos* terminator was fused with an *hpt* gene (hygromycin B phosphotransferase) controlled by the *CaMV35S* promoter and the *Nos* terminator to produce the overexpression construct *Zm908p-Zm908p11OE* (Supplementary Fig. S1H at *JXB* online). The antisense strand of the 3'-untranslated region (UTR) of *Zm908* (*Zm908p11a*), a part of the β-glucuronidase (GUS) gene (*GUS*), and the sense strand of the 3'-UTR of *Zm908* (*Zm908p11s*) were fused to generate the stem–loop fragment. The stem–loop fragment controlled by *Zm908p* and the *Nos* terminator was fused with an *hpt* gene controlled by the *CaMV35S* promoter and the *Nos* terminator to produce *Zm908p-Zm908p11Ri* (Supplementary Fig. S1I). The detailed construction is shown in the Supplementary Materials and methods.

Plant transformation

Tobacco transformation

The *35S-Zm908s*, *35S-Zm908a*, *35S-Zm908p11*, *35S-Zm908p11ss*, *35S-Zm908p11fs*, *Lat52-Zm908s*, and *Lat52-Zm908p11* constructs were transformed into tobacco (*N. tabacum* cv Samsun NN) using the leaf disc method (Horsch *et al.*, 1985). The regenerated plants were transplanted in the greenhouse at a temperature of 25 °C day/20 °C night with summer daylight and ~50% relative humidity.

Maize transformation

The *Zm908p-Zm908p11OE* and *Zm908p-Zm908p11Ri* constructs were transformed into calli induced from the immature embryos of the hybrid Z31×Q31 by particle bombardment. Resistant calli were screened by 20 mg ml^{-1} hygromycin on NB medium, as described by Wang *et al.* (2006).

Quantitative RT–PCR

Maize total RNA was extracted from root, stem, leaf, seed, different anther stages, and mature pollen using TRIzol® Reagent (Invitrogen, USA) following the manufacturer's instructions. A 2 μg aliquot of total RNA was reverse transcribed by M-MLV reverse transcriptase (Promega, USA) with oligo$(dT)_{20}$ primer. Quantitative reverse transcription–PCR (RT–PCR) was conducted using TaKaRa SYBR® Premix Ex Taq™ (TaKaRa, Japan) on a Bio-Rad Real-Time System CFX96TM C1000 thermal cycler (Bio-Rad, USA). The PCR conditions were 95 °C for 10 s, followed by 40 cycles of 94 °C for 5 s, 60 °C for 20 s, and 72 °C for 20 s. Independent biological triplicates and technical triplicates were used for each experiment. Data analysis was performed using BIO-RAD CFX Manager software (Bio-Rad, USA). The maize *Tubulin* gene was used as an internal control. The primer pair for *Zm908* was 9rtf and 9rtr, and for *Tubulin* it was trtf and trtr (Supplementary Table S1 at *JXB* online). The relative gene expression level was calculated using the $2^{-\Delta\Delta Ct}$ analysis method.

Northern blot hybridization

Total RNAs (30 μg) extracted from root, stem, leaf, uninucleate and binucleate anthers, and mature pollen using TRIzol® Reagent (Invitrogen, USA) were separated on a 1.2% agarose–formaldehyde gel, and transferred onto nylon membranes (Boehringer Mannheim, Germany). The *Zm908p11* fragment was labelled with [α-^{32}P]dCTP as a probe using the Prime-a-Gene® Labeling System (Promega, USA). The membranes were pre-hybridized for 6 h at 65 °C, and hybridization was performed for 20 h at 65 °C with labelled probes. After hybridization, membranes were washed in 2× SSC/0.5% SDS for 30 min and in 0.5× SSC/0.5% SDS for 30 min at 65 °C. Finally, the hybridization signals were recorded on an X-omat BT Film (Kodak, Japan).

In vitro *pollen germination assays*

Pollen grains were harvested from freshly opened anthers, added to 20 μl of liquid pollen germination medium, then placed onto solid pollen germination medium [10 mM $CaCl_2$, 0.05 mM KH_2PO_4, 0.01% (w/v) H_3BO_3, 0.1% (w/v) yeast extract, 10% (w/v) sucrose, and 6% (w/v) PEG-4000 solidified with 1% (w/v) agar for maize pollen; 1 mM $CaCl_2$, 1 mM $Ca(NO_3)_2{\cdot}4H_2O$, 1 mM $MgSO_4{\cdot}7H_2O$, 0.01% (w/v) H_3BO_3, and 18% (w/v) sucrose solidified with 0.5% (w/v) agar for tobacco pollen]. The plates were incubated for 3 h at 28 °C and 100% humidity in the dark. All the calculations were performed with technical triplicates and biological triplicates. At least 400 grains were used per assay. Statistical analysis was performed using Microsoft Excel.

Antiserum production, protein extraction, and western blot analysis

The antibody was produced by Beijing Protein Innovation Company, Ltd (Beijing, China; http://www.proteomics.org.cn/). A peptide corresponding to the amino acid sequence (GKWVRRGRLNPAPADC) of *Zm908p11* cDNA was synthesized, and 200 μg of the synthesized peptide was used to immunize rabbits subcutaneously. Booster shots were given at 12 d intervals with the same amount of antigen three times.

Maize total protein from root, stem, leaf, seed, and mature pollen was extracted with an extraction buffer consisting of 2.5% (w/v) sucrose, 0.1% (v/v) β-mercaptoethanol, and 5 mM potassium phosphate buffer, pH 6.0. A 20 μg aliquot of protein was separated by 19% Tricine-SDS–PAGE (Schägger, 2006), and blotted onto a polyvinylidene fluoride (PVDF) membrane (Millipore, USA). The western blot analysis was performed according to the method reported by Gallagher *et al.* (1993). The Zm908p11 antiserum was affinity purified and used as the primary antibody at a 1:1000 dilution. Alkaline phosphatase-conjugated goat anti-rabbit IgG (Promega, USA) was used as the secondary antibody (1: 5000). The signal was detected using the NBT/BCIP reaction kit (Promega, USA).

Scanning electron microscopy

Mature maize pollen grains from fresh dehiscent anthers were collected and mounted on stubs using double-sided carbon tape, and coated with palladium–gold by an ion coater (Eiko IB-3, Japan).

The specimens were examined on a scanning electron microscope (Hitachi S-3400N, Japan) at an accelerating voltage of 15 kV.

Alexander's staining assay

Alexander's staining assay was performed as previously described (Alexander, 1969). Mature pollen grains from fresh dehiscent anthers were collected and incubated with Alexander's solution for 10–15 min, and then observed by light microscopy (Leica, Germany).

Subcellular localization of Zm908p11 protein

For subcellular localization, *Zm908p11-GFP* (green fluorescent protein) was transiently transformed into tobacco pollen. For construction of *Zm908p11-GFP*, the *Zm908p11* fragment was amplified by PCR using primer pair 9Gf and 9Gr (Supplementary Table S1 at *JXB* online), and fused to the C-terminus of *GFP* in pLat52-GFP with *Eco*RI and *Kpn*I sites. Fresh pollen grains were harvested from tobacco anthers and transferred into liquid pollen germination medium. Transformation was conducted by particle bombardment. Following bombardment, the pollen grains were incubated to germinate for 3 h, at 28 °C and 100% humidity in the dark. The fluorescence of GFP was monitored using a Zeiss LSM510 (Zeiss, Germany).

Yeast two-hybrid assay

To determine proteins that interact with Zm908p11, the MATCHMAKER GAL4 Two-Hybrid System3 (Clontech, USA) was used. *Zm908p11* was amplified from pMD18-Zm908s with the primer pair y2h9Nf and y2h9Nr (Supplementary Table S1 at *JXB* online), and cloned in-frame into the *Bam*HI and *Sal*I sites of the yeast vector pGBKT7 to obtain *BD-Zm908p11* which was used as the bait. For screening of maize pollen protein that interacted with Zm908p11, the maize mature pollen cDNA library was ligated into pGADT7 as the prey. The constructs were co-transformed into yeast strain AH109, and screened on SD/–Ade/–His/–Leu/–Trp medium according to protocol. This was followed by X-α-galactosidase staining to test the interaction. For analysis of the interaction between Zm908p11 and ZmPRO1, the ORF of *ZmPRO1* was amplified from maize pollen cDNA with primer pair y2hPf and y2hPr (Supplementary Table S1), and cloned into the *Eco*RI and *Xho*I sites of pGADT7 to generate *AD-ZmPRO1*.

LCI assay

The luciferase complementation imaging (LCI) assay was performed as previously described (Chen *et al.*, 2008). The cDNA of *Zm908p11* was amplified by PCR using primers L9f and NL9r, and L9f and CL9r, and *ZmPRO1* was amplified using LPf and NLPr, and LPf and CLPr (Supplementary Table S1 at *JXB* online). They were then cloned into the *Kpn*I and *Sal*I sites of pCAMBIA-NLuc and pCAMBIA-CLuc vectors, respectively. These constructs were transformed into *Agrobacterium* strain GV3101. Bacterial suspensions were infiltrated into fully expanded leaves of the 7-week-old *N. benthamiana* plants using a needleless syringe. Plants were grown in darkness for 12 h, and then with 16 h light/8 h dark for 60 h at 22 °C. Finally, the leaves were daubed with firefly luciferase and observed with an AndoriXon camera iKon-M (Andor, USA).

Microarray analysis

Total RNA was extracted from mature pollen grains, collected from fresh dehiscent anthers of *Zm908p-Zm908p11OE* and wild-type plants, using TRIzol® Reagent (Invitrogen, USA). RNA quantity and quality were measured with a Nanodrop ND-2000 spectrophotometer (Thermo, USA). Microarray analyses were performed using Affymetrix microarray technology by CapitalBio Corporation (http://www.capitalbio.com) following the Affymetrix GeneChip® expression analysis technical manual (Affymetrix, USA). Data analysis was carried out according to the Affymetrix statistical algorithms description document (Affymetrix, USA). *P*-values between *Zm908p-Zm908p11OE* and wild-type plants were calculated by Wilcoxon's rank test (Wilcoxon, 1945). The gene expression analysis and gene ontology were performed using AgriGo (http://bioinfo.cau.edu.cn/agriGO/). Some of the differentially expressed genes were confirmed by quantitative RT–PCR using the primer pairs listed in Supplementary Table S3 at *JXB* online.

Results

Cloning and bioinformatic analysis of Zm908

Previously, a pollen-predominant cDNA fragment (682 bp) was obtained from the maize mature pollen cDNA library by differential screening using cDNA probes synthesized from the mRNA of mature maize pollen and leaf tissue (Li *et al.*, 2001). Using this cDNA fragment, two genomic clones were isolated by plaque hybridization experiments. One of these two clones, *Zm401*, has been previously described (Dai *et al.*, 2004). The other clone, which contained a 14 kb DNA fragment insertion, was digested with *Sal*I and cloned into a pGEM-3Zf (+) vector. The ~4.5 kb *Eco*RI/*Xba*I fragment was further subcloned into pGEM-3Zf (+). This clone was named *Zm908* following sequencing. The use of RT–PCR and 5' rapid amplification of cDNA ends (5'-RACE) enabled a 1758 bp full-length cDNA of *Zm908* to be cloned from mature pollen RNA.

Comparison of the *Zm908* cDNA with its genomic sequence revealed that the *Zm908* genomic clone comprises a 5'-non-coding region (225 bp), one exon (1259 bp), and a 3'-non-coding region (274 bp); it does not have any introns (Fig. 1A). This gene is located on chromosome 2 in the locus AC206253 (http://www.maizegdb.org). ORF prediction analysis of the *Zm908* cDNA sequence using biological software identified many stop codons in all three possible reading frames, and no long ORFs were identified (Fig. 1B). The longest deduced ORF is 294 bp in length (+697 to +990), and encodes a putative 97 amino acid peptide that is provisionally designated as Zm908p11 (Fig. 1C). The deduced Zm908p11 peptide has a molecular mass of 11 kDa, with an isoelectric point (pI) of 11.6. It contains a proline-rich stretch and has no predicted signal peptide at the N-terminus (http://www.cbs.dtu.dk/services/SignalP/). A BLASTn search (http://blast.ncbi.nlm.nih.gov/Blast.cgi) of *Zm908* revealed that it was only homologous to Poaceae; no homologous genes in dicots or in other monocots were identified. The phylogenetic analysis of *Zm908* using MEGA4 software is shown in Supplementary Fig. S2 at *JXB* online. *Zm908* shared 65.8% identity with *Zm401* (AY911609), 66.4% with *Setaria italica Si401* (DQ981487), 66.7% with *Oryza sativa Os401* (EU426833), and 66.7% with *Triticum aestivum Ta401* (EU426832) cDNA, suggesting that *Zm908* is a Poaceae-specific gene.

Zm908 *transcript is predominantly expressed in mature maize pollen*

The expression pattern of the *Zm908* gene was initially investigated by quantitative RT–PCR. The expression of *Zm908* was first detected at the uninucleate stages of anthers, and

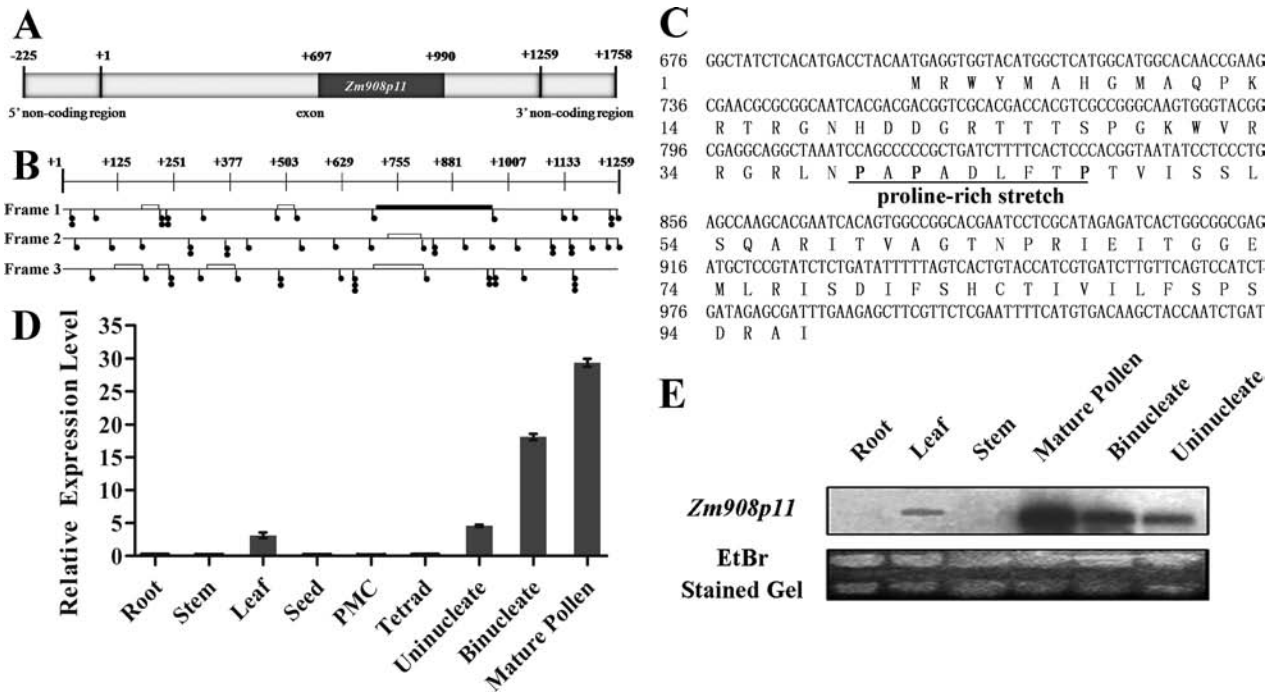

Fig. 1. Gene structure and expression patterns of *Zm908*. (A) Gene structure of *Zm908*. The longest ORF *Zm908p11* (+697 to +990) is shown by a black solid box. (B) Schematic representation of the *Zm908* cDNA sequence. Each of the three possible reading frames of *Zm908* is depicted separately. Stop codons (TAG, TAA, or TGA) are indicated by filled circles. Deduced ORFs are depicted as open boxes, and *Zm908p11* is shown by a filled box. (C) Sequence of the 97 amino acid Zm908p11 peptide; the proline-rich stretch is underlined. (D) Expression pattern of *Zm908* by quantitative RT–PCR analysis. The *y*-axis shows the relative expression level, and the *x*-axis shows different tissues. (E) Expression pattern of *Zm908* by northern blot analysis. rRNAs were used as an internal control.

increased to a peak level in mature pollen. Additionally, a weak signal for *Zm908* was detected in leaves (Fig. 1D).

To confirm the pollen-predominant expression pattern of *Zm908*, northern blot analysis was performed using an [α-^{32}P]dCTP-labelled specific sequence of cDNA as a probe. As shown in Fig. 1E, the northern blot result was consistent with that of quantitative RT–PCR. The *Zm908* transcript was detected from the uninucleate stage, and reached a maximum in mature pollen. No signal was detected in other tissues, with the exception of a weak band in the leaf. This indicated that *Zm908* may function in the late stage of pollen development and/or pollen germination and tube growth.

Zm908 *plays an important role as* Zm908p11

To investigate the function of *Zm908* during pollen development, the full-length *Zm908* cDNA was ectopically expressed in tobacco under the control of the *CaMV35S* promoter, and the *Nos* terminator (Supplementary Fig. S1A at *JXB* online). As a parallel reference, antisense *Zm908* cDNA using the same regulatory elements (Supplementary Fig. S1B) was also transformed into tobacco. Three *35S-Zm908s* lines and three *35S-Zm908a* lines were selected for further investigation. Pollen grains from wild-type and transgenic lines were stained with I_2–KI solution. The results were shown in Fig. 2. The majority of pollen grains from the *35S-Zm908s* anthers were malformed and the pollen I_2–KI staining rate was dramatically reduced. In contrast, the pollen grains from the *35S-Zm908a* anthers were round and as fully stained as those of the wild type.

Considering that the *Zm908* sequence has no long ORF, the longest ORF is 294 bp and encodes a putative 97 amino acid peptide Zm908p11. Does the *Zm908* function as Zm908p11? To answer this question, western blot analysis was performed using Zm908p11 antiserum to test for the existence of the Zm908p11 peptide in wild-type maize. Excitingly, a band at the expected size of 11 kDa was detected in mature maize pollen, but not in other tissues (Fig. 3). This indicated that the small peptide Zm908p11 is present in mature pollen.

To confirm whether the transgenic phenotypes observed in *35S-Zm908s* anthers were caused by *Zm908p11*, the construct *35S-Zm908p11* (Supplementary Fig. S1C at *JXB* online) was transformed into tobacco to produce ectopic overexpression of *Zm908p11* lines. The transgenic lines did not show any noticeable differences in vegetative and floral development. However, I_2–KI pollen grain staining revealed that only 38.2% of *35S-Zm908p11* pollen grains were normal in comparison with full-length *Zm908* transgenic tobacco (Fig. 4A, B).

To elucidate further the requirement for an intact ORF of *Zm908p11*, a site-specific mutation (*Zm908p11ss*; Supplementary Fig. S1D at *JXB* online) and a frameshift mutation (*Zm908p11fs*; Supplementary Fig. S1E) were generated and ectopically expressed in tobacco. I_2–KI staining showed that both *35S-Zm908p11ss* and *35S-Zm908p11fs* transgenic pollen grains were round and dark-stained like those of the wild type (Fig. 4A, B). This indicated that both

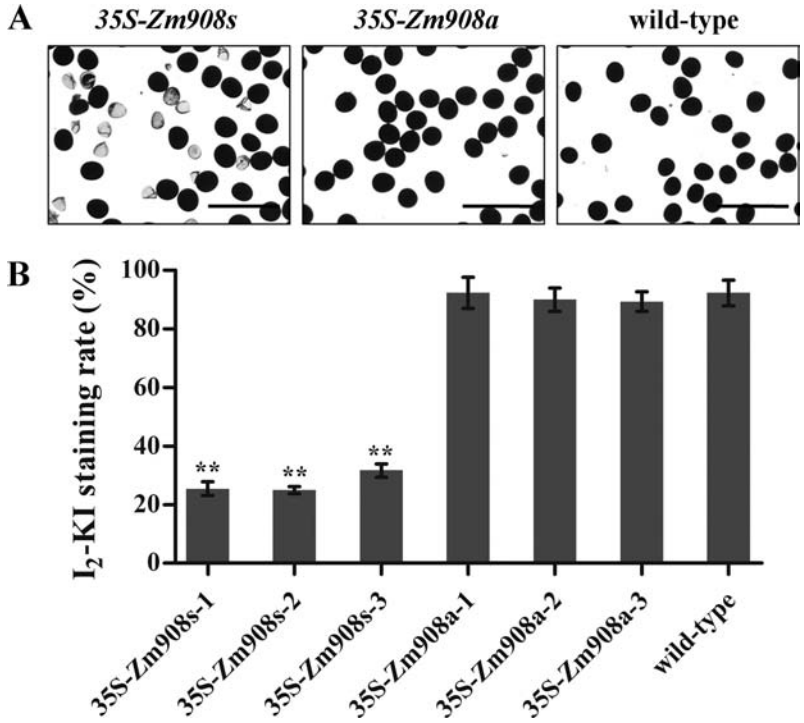

Fig. 2. Transgenic pollen grain phenotype and pollen I_2–KI staining rate analysis. Mature pollen grains were collected from wild-type and transgenic tobacco plants. (A) Tobacco pollen grains were stained with I_2–KI solution. Normal pollen grains are deeply stained with a round shape, whereas malformed pollen grains are not stainable. Bars=200 μm. (B) The mature pollen I_2–KI staining rate (%) in transgenic tobacco. *35S-Zm908s-1/2/3* and *35S-Zm908a-1/2/3* are transgenic tobacco lines. All the calculations were performed with technical triplicates and biological triplicates, and at least 400 grains were used per assay. Error bars represent the mean ±SD; $^{**}P < 0.01$ (Student's *t*-test).

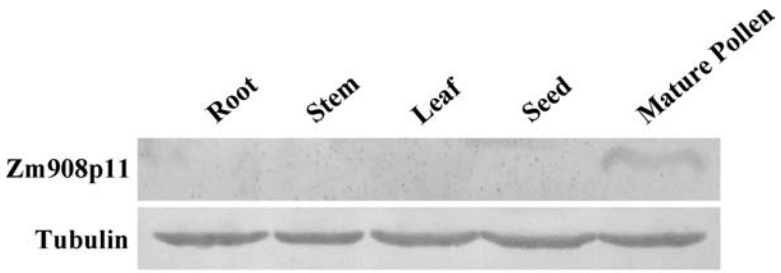

Fig. 3. Western blot analysis of Zm908p11 peptide in maize. Immunoblot of 20 μg of total protein extracted from root, stem, leaf, seed, and mature pollen loaded as indicated.

the site-specific and the frameshift mutation, which abolished production of Zm908p11 peptide, failed to show any of the phenotypic changes found in *35S-Zm908p11* transgenic lines. These results demonstrated that *Zm908* functions as Zm908p11.

To check whether the transgenic phenotypes that were found were a consequence of constitutive expression of *Zm908p11* controlled by the *CaMV35S* promoter, two constructs *Lat52-Zm908s* (Supplementary Fig. S1F at *JXB* online) and *Lat52-Zm908p11* (Supplementary Fig. S1G), controlled by the pollen-specific promoter *Lat52*, were introduced into tobacco. Unlike the transgenic lines with constitutive expression of *Zm908* and *Zm908p11*, both *Lat52-Zm908s* and *Lat52-Zm908p11* pollen showed normal I_2–KI staining (Fig. 4C), and decreased germination efficiency (15.6–18.3% for *Lat52-Zm908* and 16.5–20.1% for *Lat52-Zm908p11*) compared with wild-type pollen (93.6–98.1%, Fig. 4D, E) in an *in vitro* germination test. These results implied that Zm908p11 is functional in maize pollen germination.

Zm908p11 is localized in the cytoplasm of pollen tubes

To investigate whether Zm908p11 peptide is localized in the pollen tube, *Lat52-Zm908p11GFP* was constructed and introduced into fresh tobacco pollen grains by particle bombardment transformation. *Lat52-GFP* was used as a control. The green fluorescence signal of Zm908p11–GFP was observed throughout the pollen tube cytoplasm at the same levels as

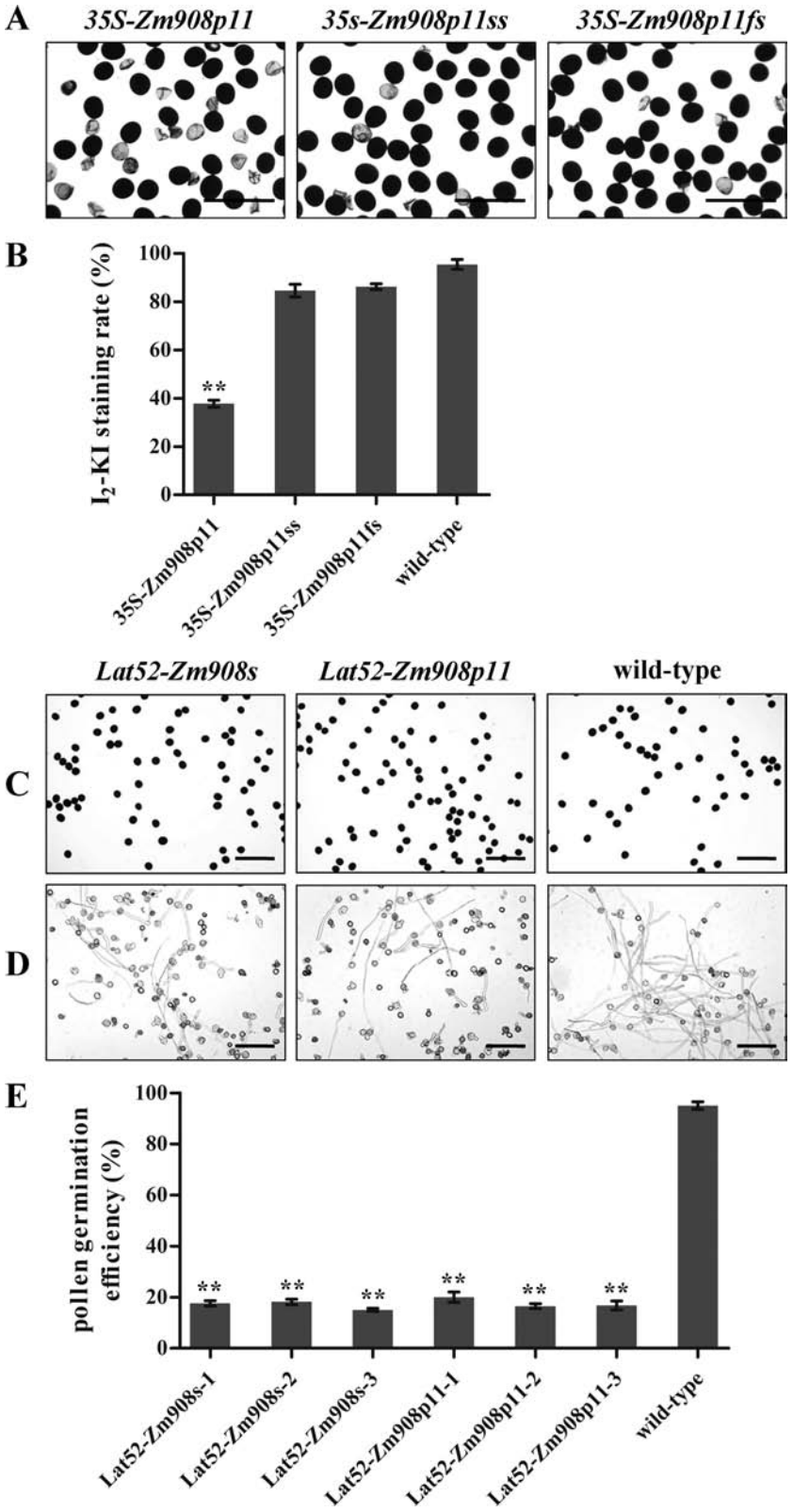

Fig. 4. Transgenic pollen grain phenotype and analysis. Mature pollen grains were collected from wild-type and transgenic tobacco plants. (A) and (C) Tobacco pollen grains were stained with I_2–KI solution. Normal pollen grains are deeply stained with a round shape, whereas malformed pollen grains are not stainable. (A) Bars=200 μm; (C) bars=250 μm. (B) The mature pollen I_2–KI staining rate (%) in transgenic tobacco. (D) *In vitro* pollen tube germination assay. Pollen grains were incubated *in vitro* for 3 h at 28 °C and 100% humidity in the dark. Bars=250 μm. (E) *In vitro* pollen germination efficiency analysis in transgenic tobacco. *Lat52-Zm908s-1/2/3* and *Lat52-Zm908p11-1/2/3* are transgenic tobacco lines. All the calculations were performed with technical triplicates and biological triplicates, and at least 400 grains were used per assay. Error bars represent the mean ±SD; $^{**}P < 0.01$ (Student's *t*-test).

free GFP (Fig. 5); this indicated that Zm908p11 peptide was distributed in the pollen tube.

Overexpression of Zm908p11 *decreases pollen germination efficiency in maize*

To analyse the function of *Zm908p11* in maize, 282 bp of the *Zm908* promoter region (*Zm908p*) was obtained from the *Zm908* genomic clone. The construct of *Zm908p* fused with *GUS* was transformed into tobacco. Five independently transgenic lines were selected to characterize promoter activity. The results showed that GUS expression was mainly detected in the mature pollen grains of the transgenic anthers (Supplementary Fig. S3 at *JXB* online). In contrast, the anthers from untransformed control plants did not show any detectable GUS activity (data not shown).

Using *Zm908p*, the plant expression constructs *Zm908p-Zm908p11OE* (Supplementary Fig. S1H at *JXB* online) and *Zm908p-Zm908p11Ri* (Supplementary Fig. S1I) were designed and transformed into maize calli by particle bombardment to generate *Zm908p11*-overexpressing and RNAi (RNA interference) transgenic plants, respectively. Quantitative RT–PCR was conducted to analyse the relative expression level of *Zm908p11* in pollen grains (Fig. 6A). Two overexpressing lines and two RNAi lines were selected for further investigation. The vegetative and reproductive development of both transgenic lines was normal. Additionally, the pollen grains were observed using scanning electron microscopy (SEM), and Alexander, I_2–KI, and 4',6-diamiaino-2-phenylindole (DAPI) staining. The results are shown in Supplementary Fig. S4 at *JXB* online. No differences were observed between the mature pollen grains from transgenic lines and those of the wild type, indicating that *Zm908p11* may not function in pollen grain development.

In vitro pollen germination assays were further carried out. Only 33.1–37.7% of pollen grains from *Zm908p11*-overexpressing anthers yielded normal pollen tubes under these conditions (Fig. 6B, C), whereas 78.3% of pollen grains from the wild type (Fig. 6B, D) and 77.2–81.2% from *Zm908p11* RNAi anthers (Fig. 6B, E) could produce normal pollen tubes. These findings indicated that *Zm908p11* may function in maize pollen germination and tube growth.

Zm908p11 interacts with ZmPRO1

Protein–protein interaction assays were performed to investigate the function of Zm908p11 further. Zm908p11 was designed as a bait to screen a prey cDNA library prepared from mature maize pollen using yeast two-hybrid assay. A maize profilin 1 (ZmPRO1, P35081.1) was identified. A yeast transformant carrying a pair of constructs (*BD-Zm908p11*/*AD-ZmPRO1*) could grow on the SD/–Trp/–Leu/–His/–Ade selection medium, indicating direct interaction of Zm908p11 and ZmPRO1. The X-α-galactosidase assay was employed to verify the results (Fig. 7A).

In addition to the yeast two-hybrid assay, the interaction between Zm908p11 and ZmPRO1 has also been verified by a firefly LCI assay (Chen *et al.*, 2008). To conduct this assay, the following pairs of constructs, *NLuc-Zm908p11*/*CLuc-ZmPRO1*, *CLuc-Zm908p11*/*NLuc-ZmPRO1*, *NLuc*/*CLuc*, *NLuc-ZmPRO1*/*CLuc*, *NLuc*/*CLuc-ZmPRO1*, *NLuc-Zm908p11*/*CLuc*, and *NLuc*/*CLuc-Zm908p11*, were designed. Each pair of constructs was transformed into *Agrobacterium* strain GV3101, followed by infiltration of tobacco (*N. benthamiana*) leaves. The pairs *NLuc-Zm908p11*/*CLuc-ZmPRO1* and *CLuc-Zm908p11*/*NLuc-ZmPRO1* generated fluorescence signals in the transformed tobacco leaf (Fig. 7B). In contrast, no fluorescent signals were detected using the negative control sets.

Transcript profiling analysis in Zm908p11-*overexpressing transgenic pollen*

Affymetrix microarray analysis was employed to explore the gene expression of *Zm908p11* transgenic maize. Total RNA extracted from mature pollen grains collected from fresh dehiscent anthers of *Zm908p-Zm908p11OE* and wild-type plants was used. Compared with wild-type pollen, 476 genes showed differential expression in *Zm908p11* transgenic pollen. Among these, 273 genes were up-regulated and 203 down-regulated (fold change ≥2). Gene ontology (GO) analysis revealed that these differentially expressed genes were involved in cellular and metabolic processes, developmental processes, and localization (Supplementary Table S2 at *JXB* online). Among the up-regulated genes, 23 genes (4.8%) belonged to the categories of developmental processes and

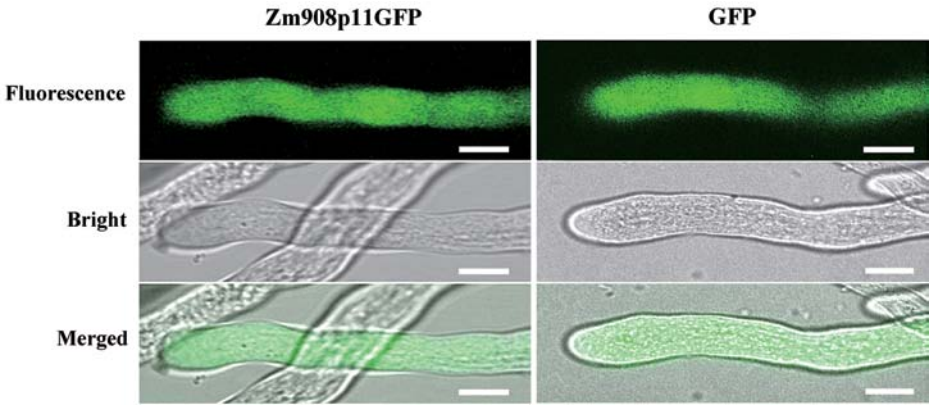

Fig. 5. Subcellular localization of Zm908p11 peptide in tobacco pollen tube *in vitro*. Bars=10 μm.

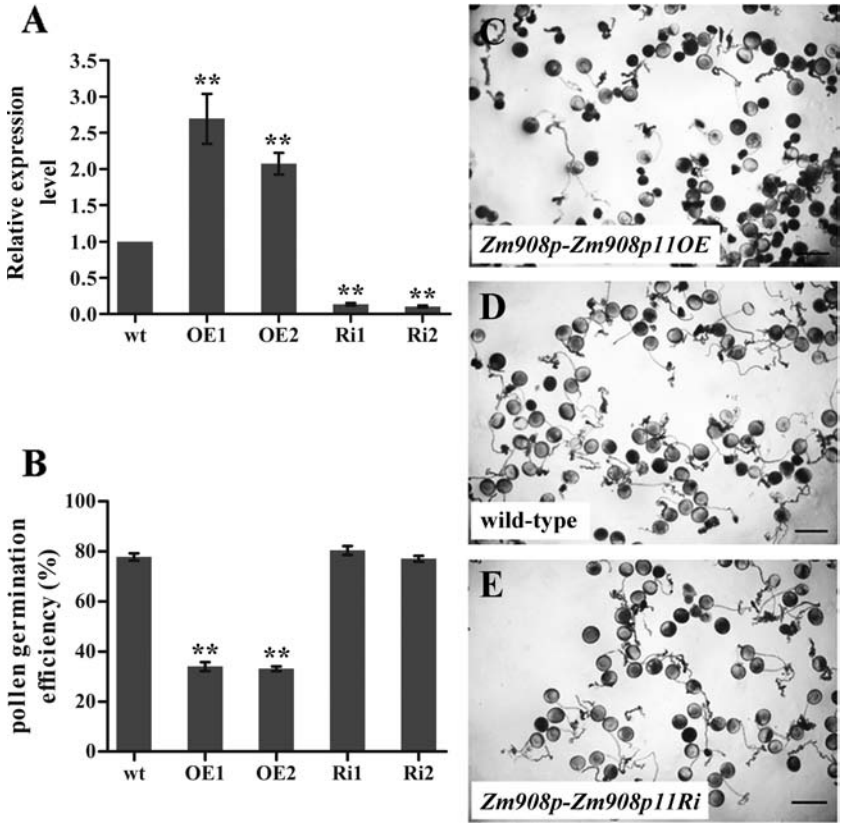

Fig. 6. Phenotypic analysis of pollen from *Zm908-Zm908p11OE, Zm908p-Zm908p11Ri*, and wild-type maize plants. (A) Relative expression level of *Zm908p11* in transgenic and wild-type maize pollen. (B) *In vitro* pollen germination efficiency of transgenic and wild-type plants. (C–E) *In vitro* germination of pollen grains from transgenic and wild-type plants. (C) Pollen grains from *Zm908p-Zm908p11OE* plants. (D) Pollen grains from wild-type plants. (E) Pollen grains from *Zm908p-Zm908p11Ri* plants. Pollen grains were cultured *in vitro* for 3 h at 28 °C and 100% humidity in the dark. Bars=100 μm. Error bars represent the mean ±SD; $^{**}P < 0.01$ (Student's *t*-test).

cellular component biogenesis, whereas 14.8% of down-regulated genes belonged to localization and establishment of localization processes.

To validate the microarray data, three up-regulated genes (AI714808, *protein phosphatase methylesterase 1*, +2.076; CD438012, *heat shock protein18c*, +2.285; and AY172634, *isoamylase-type starch debranching enzyme ISO3*, +2.001) and two down-regulated genes (AF302187, *sucrose export defective1*, –2.583; and CF021148, *CaM*, –4.78), which are involved in pollen germination and tube growth, were selected for quantitative RT–PCR analysis. The quantitative RT–PCR results confirmed the microarray data (Fig. 8).

Discussion

Zm908 *functions as Zm908p11*

Transcripts encoding sORFs are under-represented in transcriptome profiling. In maize, >8% of full-length cDNAs characterized encode ORFs of <100 amino acids and >4% encode ORFs of <40 amino acids (Soderlund *et al.*, 2009). Kastenmayer *et al.* (2006) provided the first evidence that small peptides encoded by sORF genes could be translated and are functional in *Saccharomyces cerevisiae*. These findings spur on the further investigation of small peptide genes. In this study, the focus is on a new maize small peptide, Zm908p11, encoded by an sORF gene involved in pollen germination and tube growth. Furthermore the molecular mechanisms for its function are proposed.

Previously two sORF genes, *Zm401* and *Zm908*, were obtained. Wang *et al.* (2009) demonstrated that *Zm401* actually functions as a small peptide, Zm401p10, rather than as a non-coding RNA as previously believed (Dai *et al.*, 2004, 2007). The *Zm401p10* transcript was first detected in microspores and tapetal cells at the tetrad stage of anthers, and continued to accumulate thereafter, reaching its maximum level in mature pollen. The expression of *Zm908p11* was initially weak at post-meiotic uninucleate stages, gradually increased thereafter, and reached its maximum level in mature pollen (Fig. 1D, E). Therefore, the expression patterns of these two genes are very similar in that there is low expression in early stages, building to a maximum in pollen. Overexpression of *Zm401p10* in transgenic maize under the control of the native *Zm401* promoter delayed tapetal layer degradation, and most microspores were sterile. In contrast, pollen maturation appeared to be normal in maize plants that overexpressed *Zm908p11*, but the germination efficiency of pollen grains was significantly reduced (Fig. 6B).

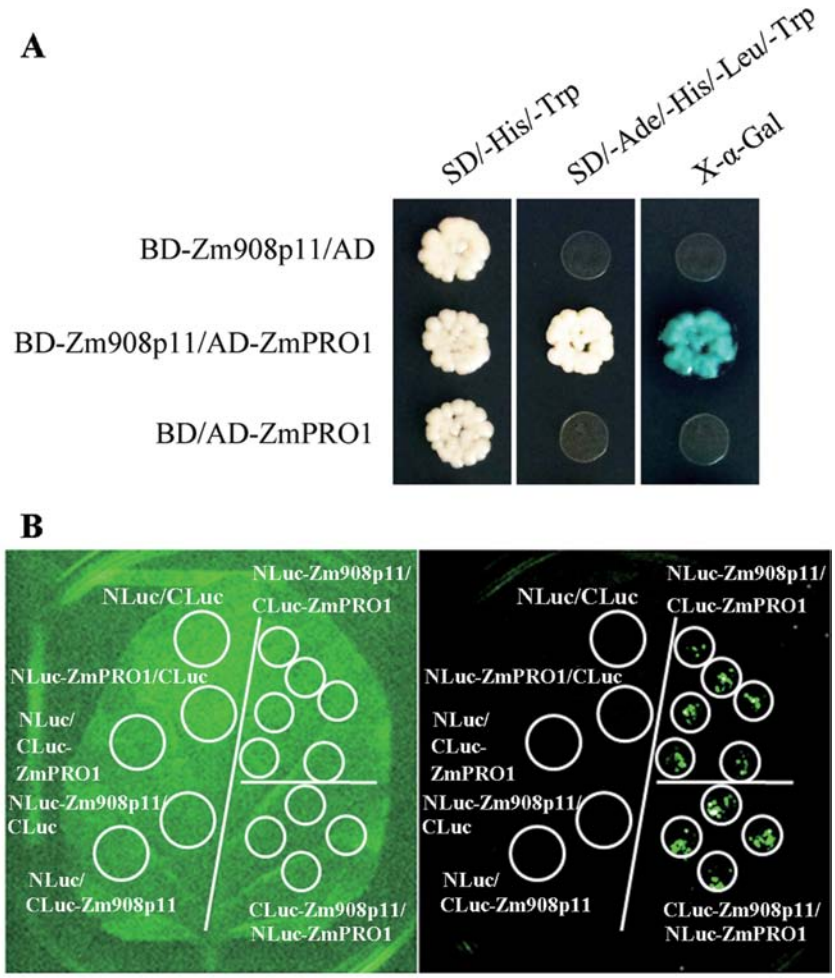

Fig. 7. Interaction of Zm908p11 with ZmPRO1. (A) Yeast two-hybrid assay. The yeast strains AH109 harbouring the construct pairs *BD-Zm908p11/AD*, *BD-Zm908p11/AD-ZmPRO1*, and *BD/AD-ZmPRO1* grow on SD/–His/–Trp and SD/–Ade/–His/–Leu/–Trp agar medium, respectively, and X-α-galactosidase assays were performed to verify protein–protein interactions. (B) LCI assay. The 7-week-old tobacco leaf was transformed by infiltration with the bacterial suspensions containing construct pairs using a needleless syringe. The left panel shows the bright field image and the right panel shows the fluorescence field image of the treated leaf.

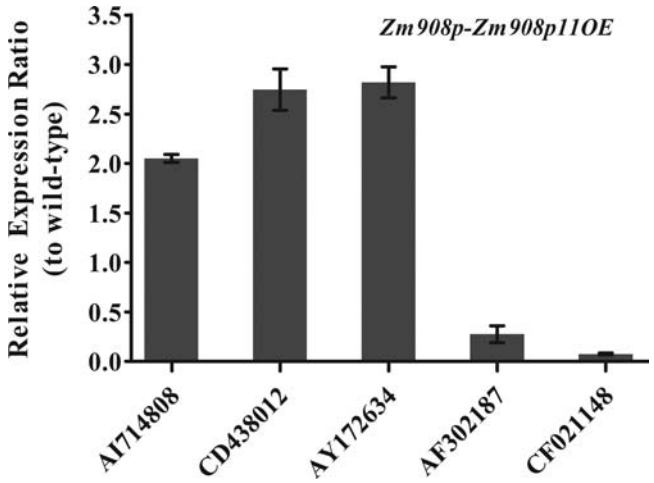

Fig. 8. Quantitative RT–PCR of five genes identified from microarray analysis. AI714808, *protein phosphatase methylesterase 1*; CD438012, *heat shock protein18c*; AY172634, *isoamylase-type starch debranching enzyme ISO3*; AF302187, *sucrose export defective1*; CF021148, *CaM*.

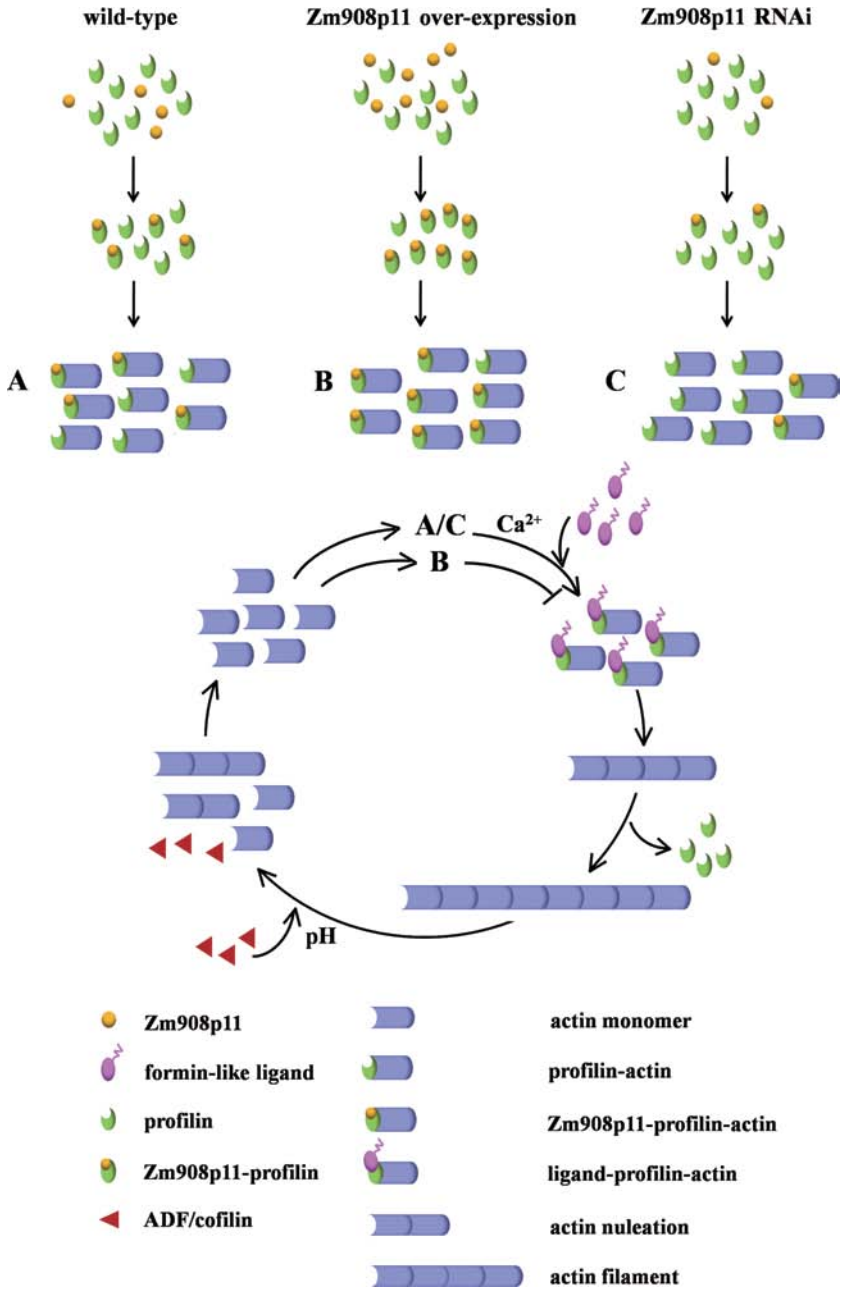

Fig. 9. A simple mechanism for Zm908p11 in regulating actin dynamics. In wild-type pollen grains, Zm908p11–profilin–actin is in dynamic equilibrium with profilin–actin. Actin nucleation occurs following the release of profilin from profilin–actin, which is triggered by the interaction between formin-like ligand and profilin, and then actin monomer adds to the barbed end of the actin filament to elongate, while Zm908p11–profilin–actin does not participate in nucleation and elongation (process A). In *Zm908p11*-overexpressing maize pollen, the increase in Zm908p11–profilin–actin may dramatically suppress the nucleation of actin filaments, or the remaining level of profilin–actin is not sufficient to maintain the elongation of actin filaments (process B). In contrast, in *Zm908p11* RNAi maize pollen, the decreased level of Zm908p11 leads to an increase in profilin–actin. Profilin–actin assembles on the barbed end of the actin filament in the presence of formin-like ligand. Thus, the actin filament nucleated and elongated, as in the wild type (process C).

The function of *Zm908* as an sORF product of Zm908p11 is based on the following evidence. First, overexpression of the full-length *Zm908* gene, controlled by *CaMV35S* or *Lat52* promoters, in tobacco caused abnormality in pollen development or tube growth. The same phenotypes were observed when the same methods were used to overexpress *Zm908p11* in tobacco (Figs 2, 4). Secondly, a protein with the expected size of Zm908p11 was detected in mature pollen by western blot analysis (Fig. 3). Finally, the pollen development of transgenic tobacco carrying constructs containing a site-specific or frameshift mutation of *Zm908p11* was the same as seen in the wild type (Fig. 4A, B). These results indicated that *Zm908* functions as Zm908p11.

Transgenic tobacco with *Zm908* or *Zm908p11* controlled by the promoters *CaMV35S* and *Lat52*, respectively, revealed different phenotypes. Pollen development was defective under the control of the *CaMV35S* promoter, whereas pollen germination efficiency was decreased and pollen development was normal under the control of the *Lat52* promoter. The distinct phenotypes may be due to the specificity of these two promoters. The genes *Zm908* and *Zm908p11* controlled by the *CaMV35S* promoter were constitutively expressed in all tissues of transgenic tobacco, whereas genes controlled by *Lat52* were exclusively expressed in pollen.

Zm908p11 interacts with profilin and may be a novel ligand involved in the regulation network of pollen tube growth

Actin dynamics are essential for pollen tube growth, and are maintained by the interaction of actin with a multitude of ABPs. Profilins can bind to actin monomers, and also bind to ligands containing a proline-rich stretch, such as formin (Mahoney *et al.*, 1999). Profilin–actin complexes are able to prevent new actin filament nucleation, which is the rate-limiting step for actin polymerization (Pollard and Cooper, 1984). While barbed ends of actin filaments are present, formins promote profilin–actin nucleation due to binding to profilin, and then new monomers continuously add to the elongating filament (Romero *et al.*, 2004).

In the present study, a proline-rich stretch was identified in Zm908p11 (Fig. 1C). The detected interaction between Zm908p11 and profilin may be a result of this structural feature. According to these results and a model for regulation of actin turnover reviewed by Staiger *et al.* (2010), the following scenario for Zm908p11 in the regulation of pollen tube growth is proposed (Fig. 9). In wild-type pollen grains, it is suggested that a normal level of Zm908p11–profilin–actin is in dynamic equilibrium with profilin–actin. Zm908p11–profilin–actin is more stable and prevents actin nucleation. Once the pollen tube grows, actin nucleation occurs following the release of profilin from profilin–actin, which is triggered by the interaction between formin-like ligand and profilin, and then actin monomer adds to the barbed end of the actin filament to elongate, while Zm908p11–profilin–actin does not participate in nucleation and elongation (Fig. 9, process A).

In *Zm908p11*-overexpressing maize, the increased level of Zm908p11 disturbs the dynamic equilibrium between profilin–actin and Zm908p11–profilin–actin. The increase in Zm908p11–profilin–actin may dramatically suppress the nucleation of actin filaments, or the remaining level of profilin–actin may not be sufficient to maintain the elongation of actin filaments. Therefore, the deficiency of pollen germination and pollen tube growth was observed in overexpressing maize (Fig. 9, process B). In contrast, in *Zm908p11* RNAi maize, the decreased level of Zm908p11 leads to an increase of profilin–actin. Profilin–actin assembles on the barbed end of the actin filament in the presence of formin-like ligand. Thus, the actin filament was nucleated and elongated, as in the wild type, resulting in the normal growth of pollen tubes (Fig. 9, process C).

It is possible that *Zm908* may also act as a signalling factor to regulate gene expression in plants. Therefore, microarray technology was used to analyse the gene expression patterns of *Zm908p11*-overexpressing maize. This identified 203 genes as being down-regulated, including several genes that are involved in pollen tube growth. An example of a significantly down-regulated gene is *CaM* (CF021148, fold change: –4.78); this shares 97–99% identity with *Arabidopsis CaM* genes. CaM is a small conserved Ca^{2+}-binding protein and has no enzymatic activity. After binding to Ca^{2+}, the complex can modulate many downstream cellular target proteins, and this leads to a series of different physiological responses (Snedden and Fromm, 1998, 2001). In the *Arabidopsis cam2-2* mutant, pollen germination efficiency was reduced nearly 30% compared with the wild type *in vitro* (Landoni *et al.*, 2010).

In conclusion, a novel maize small peptide Zm908p11 was identified which plays a required role during pollen tube growth. Zm908p11 may be a ligand of profilins to prevent profilin–actin nucleation. Additionally, it may participate in a molecular network in association with pollen tube development.

Supplementary data

Supplementary data are available at *JXB* online.

Figure S1. Diagram of the constructs used in the present study.

Figure S2. Phylogenetic analysis of *Zm908*.

Figure S3. GUS staining of pollen grains and anther from *Zm908p-GUS* transgenic tobacco.

Figure S4. Phenotypic analysis of pollen grains from *Zm908-Zm908p11OE*, *Zm908p-Zm908p11Ri*, and wild-type maize.

Table S1. List of primers used for gene cloning and quantitative RT–PCR assays.

Table S2. List of genes up-regulated and down-regulated which were changed ≥2-fold in the microarray analysis.

Table S3. List of primers used for microarray analysis.

Acknowledgements

We are grateful to Dr Zhen Su (China Agricultural University) for assisting with the Affymetrix GeneChip analysis; Dr Ying Fu (China Agricultural University) for help with protein localization in the pollen tube; Dr Dapeng Zhang (Tsinghua University) for help with the LCI assay; and Haihong Liu and Junzhen Jia at the '985' Technology Platform (China Agricultural University) for their assistance in scanning electron microscopy. We also thank Dr Virginia Walbot (Stanford University, USA) and Dr Roger B. Deal (Emory University, USA) for their kind reviews. This work was supported by research grants from the Natural Science Foundation of China (grant no. 30971555) and the National Basic Research Program of China (2012CB215301).

References

Alexander MP. 1969. Differential staining of aborted and nonaborted pollen. *Stain Technology* **44,** 117–122.

Borg M, Brownfield L, Twell D. 2009. Male gametophyte development: a molecular perspective. *Journal of Experimental Botany* **60,** 1465–1478.

Butenko MA, Patterson SE, Grini PE, Stenvik GE, Amundsen SS, Mandal A, Aalen RB. 2003. *INFLORESCENCE DEFICIENT IN ABSCISSION* controls floral organ abscission in Arabidopsis and identifies a novel family of putative ligands in plants. *The Plant Cell* **15,** 2296–2307.

Cárdenas L, Lovy-Wheeler A, Wilsen KL, Hepler PK. 2005. Actin polymerization promotes the reversal of streaming in the apex of pollen tubes. *Cell Motility and the Cytoskeleton* **61,** 112–127.

Chen CY, Wong EI, Vidali L, Estavillo A, Hepler PK, Wu H-m, Cheung AY. 2002. The regulation of actin organization by actin-depolymerizing factor in elongating pollen tubes. *The Plant Cell* **14,** 2175–2190.

Chen H, Zou Y, Shang Y, Lin H, Wang Y, Cai R, Tang X, Zhou JM. 2008. Firefly luciferase complementation imaging assay for protein–protein interactions in plants. *Plant Physiology* **146,** 368–376.

Chen YF, Matsubayashi Y, Sakagami Y. 2000. Peptide growth factor phytosulfokine-α contributes to the pollen population effect. *Planta* **211,** 752–755.

Cheung AY, Chen CY-h, Glaven RH, de Graaf BHJ, Vidali L, Hepler PK, Wu H-m. 2002. Rab2 GTPase regulates vesicle trafficking between the endoplasmic reticulum and Golgi bodies and is important to pollen tube growth. *The Plant Cell* **14,** 945–962.

Chu CC, Wang CC, Sun CS, Hsn C, Yin KC, Chu CY, Bi FY. 1975. Establishment of an efficient medium for anther culture of rice through comparative experiments on the nitrogen sources. *Scientia Sinica* **18,** 659–668.

Clark SE, Running MP, Meyerowitz EM. 1995. *CLAVATA3* is a specific regulator of shoot and floral meristem development affecting the same processes as *CLAVATA1*. *Development* **121,** 2057–2067.

Dai XY, Yu JJ, Ao GM, Zhao Q. 2007. Overexpression of *Zm401*, an mRNA-like RNA, has distinct effects on pollen development in maize. *Plant Growth Regulation* **52,** 229–239.

Dai XY, Yu JJ, Zhao Q, Zhu DY, Ao GM. 2004. Non-coding RNA for *ZM401*, a pollen-specific gene of *Zea mays*. *Acta Botanica Sinica* **46,** 497–504.

Fedorov AA, Magnus KA, Graupe MH, Lattman EE, Pollard TD, Almo SC. 1994. X-ray structures of isoforms of the actin binding protein profilin that differ in their affinity for phosphatidylinositol phosphates. *Proceedings of the National Academy of Sciences, USA* **91,** 8636–8640.

Fletcher JC, Brand U, Running MP, Simon R, Meyerowitz EM. 1999. Signaling of cell fate decisions by *CLAVATA3* in *Arabidopsis* shoot meristems. *Science* **283,** 1911–1914.

Gallagher S, Winston SE, Fuller SA, Hurrell JGR. 1993. Immunoblotting and immunodetection. In: Ausubel FM, Brent R, Kingston RE, Moore DD, Sedtman JG, Smith JA, Struhl K, eds. *Current protocols in molecular biology* , Vol. **2**. New York: John Wiley & Sons, 10.8.1–10.8.16.

Gibbon BC, Zonia LE, Kovar DR, Hussey PJ, Staiger CJ. 1998. Pollen profilin function depends on interaction with proline-rich motifs. *The Plant Cell* **10,** 981–994.

Higaki T, Sano T, Hasezawa S. 2007. Actin microfilament dynamics and actin side-binding proteins in plants. *Current Opinion in Plant Biology* **10,** 549–556.

Holdaway-Clarke TL, Hepler PK. 2003. Control of pollen tube growth: role of ion gradients and fluxes. *New Phytologist* **159,** 539–563.

Horsch RB, Fry JE, Hoffmann NL, Eichholtz D, Rogers SG, Fraley RT. 1985. A simple and general method for transferring genes into plants. *Science* **227,** 1229–1231.

Kadota A, Yamada N, Suetsugu N, Hirose M, Saito C, Shoda K, Ichikawa S, Kagawa T, Nakano A, Wada M. 2009. Short actin-based mechanism for light-directed chloroplast movement in *Arabidopsis*. *Proceedings of the National Academy of Sciences, USA* **106,** 13106–13111.

Kang F, Purich DL, Southwick FS. 1999. Profilin promotes barbed-end actin filament assembly without lowering the critical concentration. *Journal of Biological Chemistry* **274,** 36963–36972.

Kastenmayer JP, Ni L, Chu A, *et al.* 2006. Functional genomics of genes with small open reading frames (sORFs) in *S. cerevisiae*. *Genome Research* **16,** 365–373.

Kim H, Park M, Kim SJ, Hwang I. 2005. Actin filaments play a critical role in vacuolar trafficking at the Golgi complex in plant cells. *The Plant Cell* **17,** 888–902.

Kovar DR, Drobak BK, Staiger CJ. 2000. Maize profilin isoforms are functionally distinct. *The Plant Cell* **12,** 583–598.

Kovar DR, Harris ES, Mahaffy R, Higgs HN, Pollard TD. 2006. Control of the assembly of ATP- and ADP-actin by formins and profilin. *Cell* **124,** 423–435.

Landoni M, Francesco AD, Galbiati M, Tonelli C. 2010. A loss-of-function mutation in *Calmodulin2* gene affects pollen germination in *Arabidopsis thaliana*. *Plant Molecular Biology* **74,** 235–247.

Li C, Liu J, Yu JJ, Zhao Q, Ao GM. 2001. Cloning and expression analysis of pollen-specific cDNA ZM401 from *Zea m*ays. *Journal of Agricultural Biotechnology* **9,** 374–377.

Lopez I, Anthony RG, Maciver SK, Jiang C-J, Khan S, Weeds AG, Hussey PJ. 1996. Pollen specific expression of maize genes encoding actin depolymerizing factor-like proteins. *Proceedings of the National Academy of Sciences, USA* **93,** 7415–7420.

Ma JX, Yan BX, Qu YY, Qin FF, Yang YT, Hao XJ, Yu JJ, Zhao Q, Zhu DY, Ao GM. 2008. *Zm401*, a short-open reading-frame mRNA or noncoding RNA, is essential for tapetum and microspore development and can regulate the floret formation in maize. *Journal of Cellular Biochemistry* **105,** 136–146.

Mahoney NM, Rozwarski DA, Fedorov E, Fedorov AA, Almo SC. 1999. Profilin binds proline-rich ligands in two distinct amide backbone orientations. *Nature Structural Biology* **6,** 666–671.

Mascarenhas JP. 1990. Gene activity during pollen development. *Annual Review of Plant Physiology and Plant Molecular Biology* **41,** 317–338.

Miller DD, Lancelle SA, Hepler PK. 1996. Actin filaments do not form a dense meshwork in *Lilium longiflorum* pollen tube tips. *Protoplasma* **195,** 123–132.

Moutinho A, Hussey PJ, Trewavas AJ, Malhó R. 2001. cAMP acts as a second messenger in pollen tube growth and reorientation. *Proceedings of the National Academy of Sciences, USA* **98,** 10481–10486.

Moutinho A, Love J, Trewavas AJ, Malhó R. 1998. Distribution of calmodulin protein and mRNA in growing pollen tubes. *Sexual Plant Reproduction* **11,** 131–139.

Murashige T, Skoog F. 1962. A revised medium for rapid growth and bio assays with tobacco tissue cultures. *Physiologia Plantarum* **15,** 473–497.

Perelroizen I, Didry D, Christensen H, Chua NH, Carlier MF. 1996. Role of nucleotide exchange and hydrolysis in the function of profilin in actin assembly. *Journal of Biological Chemistry* **271,** 12302–12309.

Pollard TD, Cooper JA. 1984. Quantitative analysis of the effect of *Acanthamoeba* profilin on actin filament nucleation and elongation. *Biochemistry* **23,** 6631–6641.

Reinhard M, Giehl K, Abel K, Haffner C, Jarchau T, Hoppe V, Jockusch BM, Walter U. 1995. The proline-rich focal adhesion and microfilament protein VASP is a ligand for profilins. *EMBO Journal* **14,** 1583–1589.

Romero S, Clainche CL, Didry D, Egile C, Pantaloni D, Carlier M-F. 2004. Formin is a processive motor that requires profilin to accelerate actin assembly and associated ATP hydrolysis. *Cell* **119,** 419–429.

Schägger H. 2006. Tricine–SDS–PAGE. *Nature Protocols* **1,** 16–22.

Snedden WA, Fromm H. 1998. Calmodulin, calmodulin-related proteins and plant responses to the environment. *Trends in Plant Science* **3,** 299–304.

Snedden WA, Fromm H. 2001. Calmodulin as a versatile calcium signal transducer in plants. *New Phytologist* **151,** 35–66.

Soderlund C, Descour A, Kudrna D, *et al.* 2009. Sequencing, mapping, and analysis of 27,455 maize full-length cDNAs. *PLoS Genetics* **5,** e1000740.

Staiger CJ, Gibbon BC, Kovar DR, Zonia LE. 1997. Profilin and actin depolymerizing factor: modulators of actin organization in plants. *Trends in Plant Science* **2,** 275–281.

Staiger CJ, Goodbody KC, Hussey PJ, Valenta R, Drøbak BK, Lloyd CW. 1993. The profilin multigene family of maize: differential expression of three isoforms. *The Plant Journal* **4,** 631–641.

Staiger CJ, Poulter NS, Henty JL, Franklin-Tong VE, Blanchoin L. 2010. Regulation of actin dynamics by actin-binding proteins in pollen. *Journal of Experimental Botany* **61,** 1969–1986.

Taylor LP, Hepler PK. 1997. Pollen germination and tube growth. *Annual Review of Plant Physiology and Plant Molecular Biology* **48,** 461–491.

Vidali L, McKenna ST, Hepler PK. 2001. Actin polymerization is essential for pollen tube growth. *Molecular Biology of the Cell* **12,** 2534–2545.

Wang DX, Li CX, Zhao Q, Zhao LN, Wang MZ, Zhu DY, Ao GM, Yu JJ. 2009. *Zm401p10*, encoded by an anther-specific gene with short open reading frames, is essential for tapetum degeneration and anther development in maize. *Functional Plant Biology* **36,** 73–85.

Wang DX, Zhao Q, Zhu DY, Ao GM, Yu JJ. 2006. Particle-bombardment-mediated co-transformation of maize with a lysine rich protein gene (*sb401*) from potato. *Euphytica* **150,** 75–85.

Wilcoxon F. 1945. Individual comparisons by ranking methods. *Biometrics Bulletin* **1,** 80–83.

Yang H, Matsubayashi Y, Nakamura K, Sakagami Y. 1999. *Oryza sativa PSK* gene encodes a precursor of phytosulfokine-α, a sulfated peptide growth factor found in plants. *Proceedings of the National Academy of Sciences, USA* **96,** 13560–13565.

Zigmond SH. 2004. Formin-induced nucleation of actin filaments. *Current Opinion in Cell Biology* **16,** 99–105.